

Studies on the Stretching of Polypropylene Film. II. Polyaxial Stretching

SABURO OKAJIMA and KEISUKE HOMMA, *Faculty of Technology, Tokyo Metropolitan University, Setagaya-ku, Tokyo, Japan*

Synopsis

Polypropylene film was stretched polyaxially at 100–160°C., and the orientation behavior was studied by means of optical and x-ray method. The molecular chains oriented progressively to the film surface with an increase in stretching area v_A in the range 1–16, and the (040) selective uniplanar orientation developed at the extreme stretching. The plot of orientation versus v_A was less steep when the stretching was carried out at higher temperature, but the final degree of orientation was independent of the temperature, because the final v_A increased with temperature. At 160°C. pre-melting occurred to such a degree that the high stretching and, consequently, the high orientation could not be obtained. The orientation of the amorphous chains was always behind that of the crystalline region. In the initial stage the polyaxial stretching was not as effective in attaining high biaxial orientation as the two-step biaxial stretching, but the final orientation was the same in both types of stretching because v_A reached a value of 16 in the polyaxial stretching while it was only 2 in biaxial stretching.

INTRODUCTION

Polypropylene film was stretched polyaxially and the orientation behavior was investigated by means of optical and x-ray methods. The results were compared with those of the two-step biaxial stretching reported in the previous paper.¹

EXPERIMENTAL METHODS

Sample

The sample of polypropylene film was the same one used in Part I of this series.¹

Method of Stretching

Polyaxial stretching was carried out with apparatus A or B, shown in Figures 1 and 2 respectively. Preheating and quenching of the film were carried out as in the previous studies.

Method A. A piece of film F, 15 × 15 cm., was set on a frame R of an apparatus shown in Figure 1, which was plunged into a poly(ethylene glycol) bath thermostatted at the desired temperature, and after a 5-min.

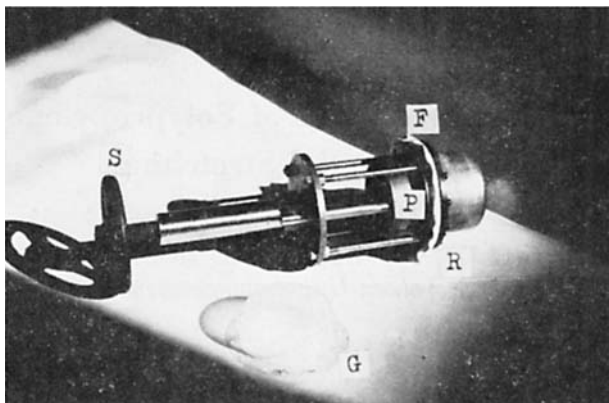


Fig. 1. Apparatus A: (F) film; (G) stretched film detached from the apparatus; (P) punch; (S) hand screw; (R) frame.

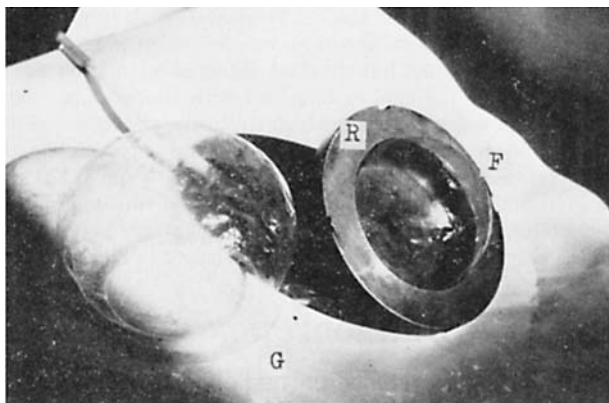


Fig. 2. Apparatus B: (F) film blown directly without using a rubber sheet; (R) ring frame; (G) blown film detached from the apparatus.

preheating the punch P was forced against F by means of a hand screw S. The portion of F in contact with the front surface of P was stretched radially (polyaxially), and the specimens for the following tests were cut out from the center of this portion.

Method B. A piece of film F, 20×20 cm., was mounted tightly on a ring frame R with a rubber sheet (a film was blown directly without the rubber sheet in Fig. 2), soaked in the bath and was blown after the preheating by applying a pressure inside the apparatus. The degree of blowing was varied by controlling the pressure. A test piece was cut out from the apex of the blown film.

In all cases the degree of stretching was expressed by the degree of expansion in area, v_A , which is expressed by D_0/D , where D_0 and D are the film thicknesses before and after the stretching or blowing, respectively. The thickness of the film was measured with a micrometer to 0.1μ .

The weakness of both types of apparatus is that the actual rate of stretching of the portion taken as the test piece cannot be known exactly. The actual rate of expansion in the following experiments is estimated to be 300%/min.

X-Ray Method

The experiment was carried out in a way similar to the previous study.¹ In order to expose film with the surface parallel to the incident x-ray beam, narrow specimens with the long sides parallel to the radial direction of the stretched film were cut out and stacked parallel but at random around the *ss* axis, the normal to the film surface.

The degree of orientation of the *c* axis with respect to the *ss* axis was evaluated from the (110) and (040) orientation after Wilchinsky.² For this purpose the degree of orientation of each plane was calculated by eq. (1) where $\langle \cos^2 \phi \rangle$ was obtained from the azimuthal scanning curve of the (110) or (040) arc. ϕ is the angle between the *ss* axis and the plane normal.

$$f_x = \frac{3}{2} \langle \cos^2 \phi \rangle - \frac{1}{2} \quad (1)$$

The crystalline diffraction was separated from the amorphous diffraction and corrected for air and incoherent scattering. The amorphous diffraction curve was prepared by tracing the minimum intensity points on the azimuthal scanning curves at various 2θ values of a sample of the highest monoaxial orientation. It is nearly coincident with the meridional scanning curve.

RESULTS AND DISCUSSION

Optical Investigation

Figure 3 gives Δn_{ss} versus v_A and d versus v_A obtained by use of apparatus A at 100, 120, 130, 140, 150, and 157°C., where d is the density and Δn_{ss} is the birefringence of the film expressed by eq. (2),

$$\Delta n_{ss} = n_{ss} - \frac{1}{2} (n_{pp} + n_{ps}) \quad (2)$$

n_{pp} , n_{ps} and n_{ss} being the refractive indices parallel to the machine direction (*pp*), in the transverse direction (*ps*), and the normal to the original film surface (*ss*), respectively. n_{pp} values of the stretched films were not always exactly equal to their n_{ps} , and the difference amounted at most to 0.004 in a few cases. The observed points scatter considerably around the mean value, as shown in the cases at 120 and 150°C., so the points were omitted from the other curves in order to avoid overcrowding.

It is clearly seen from Figure 3 that the shapes of the curve at each temperature are similar in type and the increase in $-\Delta n_{ss}$ is steep until $v_A = 2$ and slows down thereafter. This slowdown occurs at comparatively smaller v_A and lower Δn_{ss} when the stretching temperature is higher. All

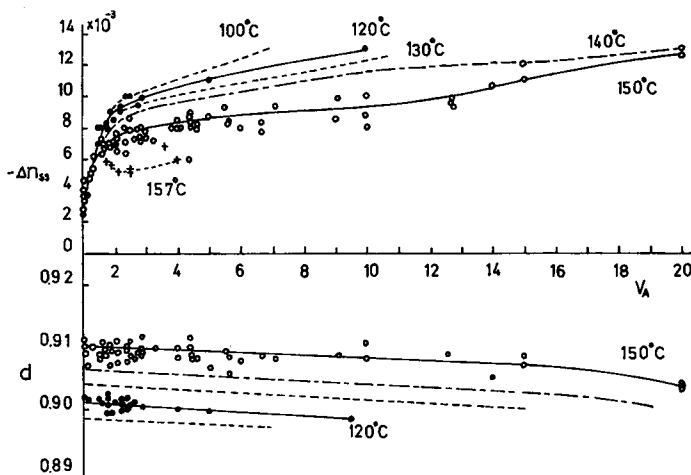


Fig. 3. Δn_{ss} vs. v_A and d vs. v_A obtained with the apparatus A.

the final Δn_{ss} values approach -13×10^{-3} and are nearly constant irrespective of the temperature of stretching, with an exception of the 157°C . stretching, where the ultimate v_A is too low due to premelting.¹ It is noteworthy that 55–75% of the ultimate Δn_{ss} is attained when $v_A = 2$, and a further increase in v_A up to 7–20 contributes only to the addition of 45–25% of the ultimate Δn_{ss} .

The intrinsic double refraction of the ideally crystalline and amorphous polypropylene, Δn_c^0 , and Δn_a^0 , cannot be said to be determined unambiguously and the various values have been reported as listed in Table I. Stein³ calculated Δn_c^0 from bond polarizability but the obtained values differed markedly, depending on whether the data of Denbigh⁴ or of Bunn and Daubeny⁵ were taken for the bond polarizability as shown in Table I. Because of this uncertainty, a value of 41.5×10^{-3} for Δn_c^0 was used in the present study. Then Δn_a^0 is $41.5 \times 10^{-3} \times 0.870/d_c = 38.5 \times 10^{-3}$, and Δn^0 , the corresponding value at $d = 0.900 \text{ g./cm.}^3$, is $41.5 \times 10^{-3} \times 0.900/d_c = 40.0 \times 10^{-3}$.

TABLE I
Birefringence of Polypropylene

	Value	Remark	Reference
Δn_c^0	0.0705	Calculated	3
Δn_c^0	0.0152	Calculated	3
Δn_c^0	0.0331	Observed	6
Δn_c^0	0.0475	Extrapolated	7
Δn_c^0	0.0415	Extrapolated	8
Δn_a^0	0.0468	Observed	6
Δn_{max}	0.034	Observed	9
Δn_{max}	0.041	Observed	7
Δn_{max}	0.041	Observed	10

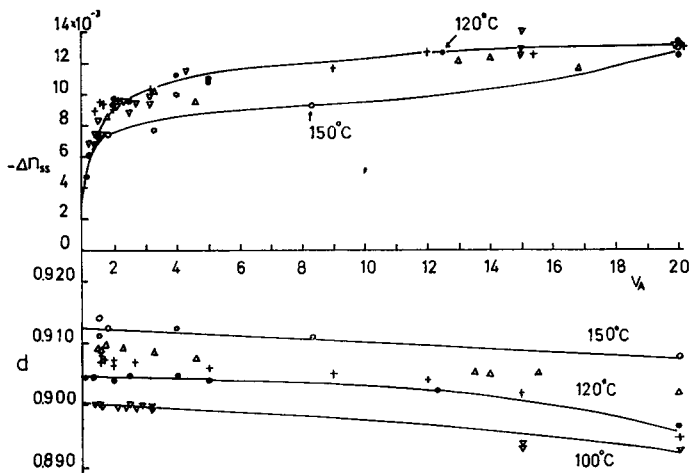


Fig. 4. Δn_{ss} vs. v_A and d vs. v_A obtained with the apparatus B at various stretching temperatures: (∇) 100°C.; (\bullet) 120°C.; (+) 130°C.; (Δ) 140°C.; (\circ) 150°C.

Then Δn_{ss}^0 , the Δn_{ss} value of a film with ideal uniplanar orientation, has a value of -20×10^{-3} according to eq. (3)

$$\Delta n_{ss}^0 = n_\gamma - \frac{1}{2}(n_\alpha + n_\gamma) = -\frac{1}{2}(n_\gamma - n_\alpha) = -\frac{1}{2}\Delta n^0 \quad (3)$$

where n_α and n_γ are the principal refractive indices of polypropylene. So the observed ultimate $\Delta n_{ss} = -13 \times 10^{-3}$ seems to be far from Δn_{ss}^0 . This may be due to the lower orientation of the amorphous chains (see below).

Figure 4 shows the results obtained with apparatus B. The trend is similar to that shown in Figure 3.

Density

The density of the film increases as the stretching temperature is elevated. The stretching itself exerts little effect upon the density, but when v_A becomes larger than 10 the density appears to decrease slightly. This trend resembles that of restretching as described in the preceding paper.¹

X-Ray Investigation

Diffraction photographs of the variously stretched films are reproduced in Figure 5, where the symbols (\parallel) and (\perp) indicate that the incident x-ray beam was parallel and perpendicular to the film surface, respectively. The diffraction patterns obtained with the x-ray beam perpendicular to the film are Debye-Scherrer type of uniform intensity, because the test specimens were prepared by stacking the test pieces at random around the ss axis.

Figure 5a indicates that the crystallite orientation was isotropic in the original film after a 5-min. preheat. In the patterns obtained with the

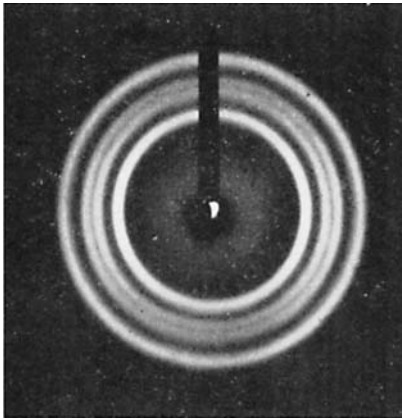
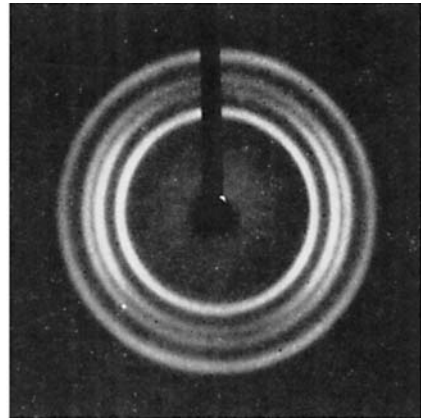
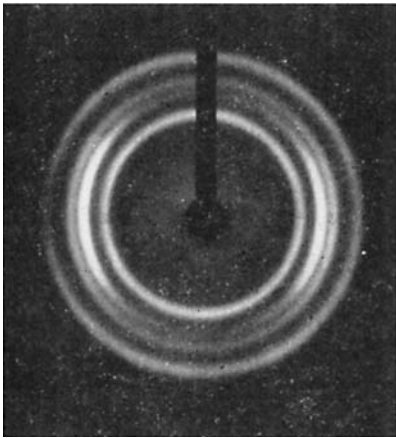
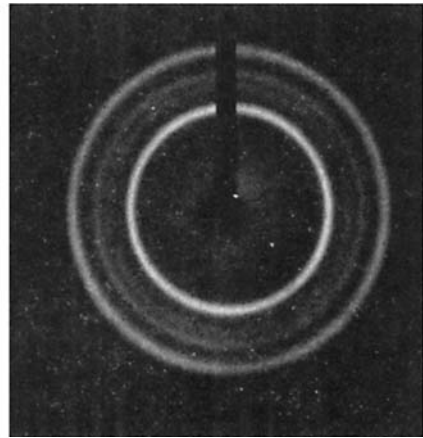
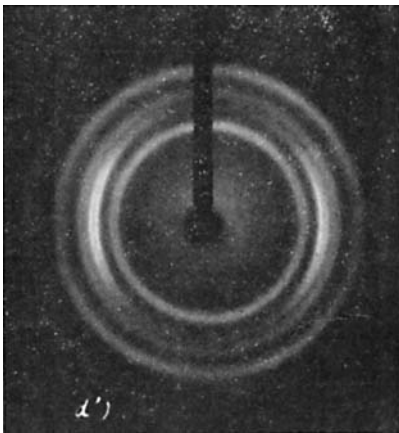
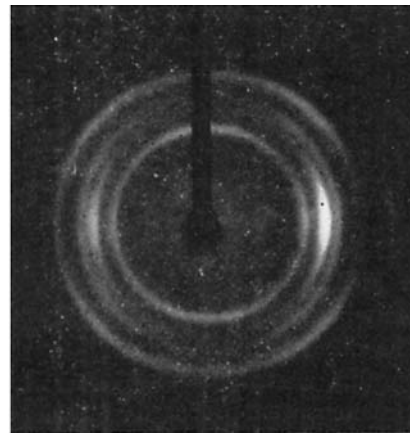
 $a (||)$  $b (||)$  $c (||)$  $c' (\perp)$  $d (||)$  $e (||)$

Fig. 5. See caption, p. 417.

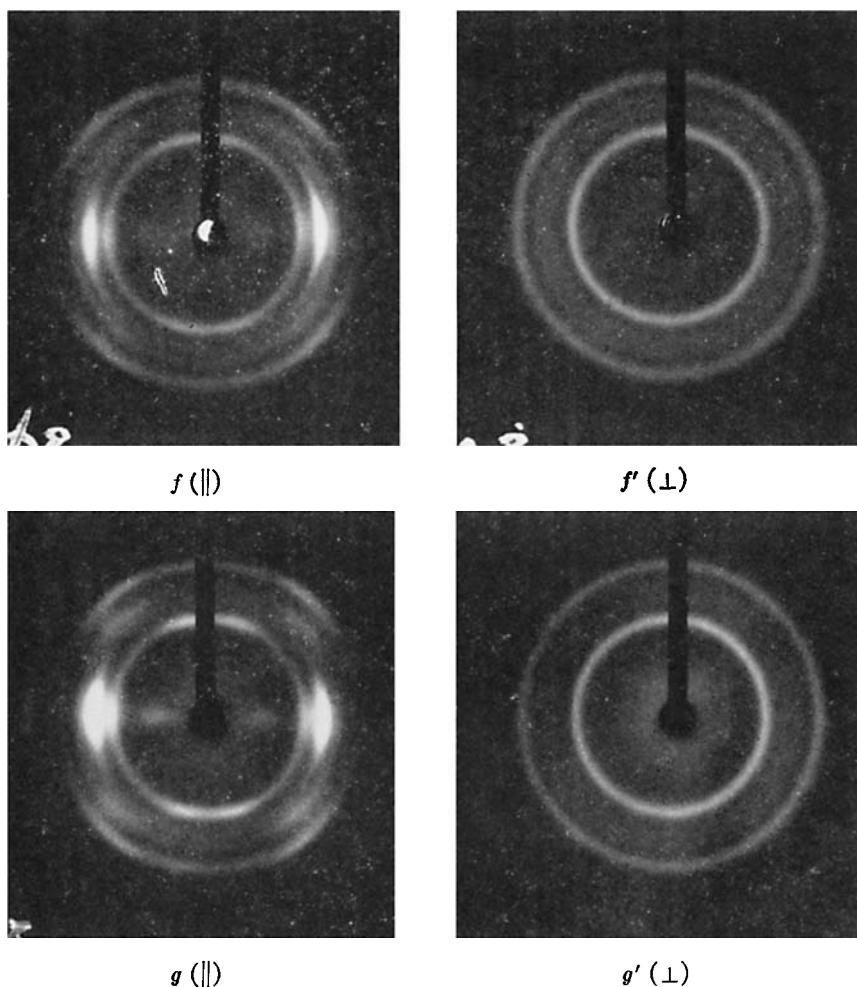


Fig. 5. X-ray diffraction photographs of the variously stretched films: The symbols (\parallel) and (\perp) indicate the incident x-ray beam parallel and perpendicular to the film surface, respectively. (a) preheated for 5 min. at 150°C ., no stretching; (b) stretching at 150°C ., $v_A = 1.7$, apparatus A, $-\Delta n_{ss} = 6.8 \times 10^{-3}$; (c), (c') stretching at 150°C ., $v_A = 3.9$, apparatus A, $-\Delta n_{ss} = 8.4 \times 10^{-3}$; (d) stretching at 150°C ., $v_A = 6.0$, apparatus A, $-\Delta n_{ss} = 9.1 \times 10^{-3}$; (e) stretching at 150°C ., $v_A > 10$, apparatus A, $-\Delta n_{ss} = 12 \times 10^{-3}$. (f), (f') stretching at 130°C ., $v_A > 10$, apparatus A. (g), (g') stretching at 100°C ., $v_A > 10$, apparatus B.

x-ray beam parallel to the film, the (040) diffraction ring splits into arcs which narrow toward the equator as v_A increases, while the change in the (110) diffraction is more complex, i.e., it appears to concentrate on the equator and the meridian (Figs. 5e-5g).

It is concluded from the optical behavior described above that the film approaches a uniplanar orientation at high stretching, where the c axis lies parallel to the film surface. Of course, uniplanar orientation cannot

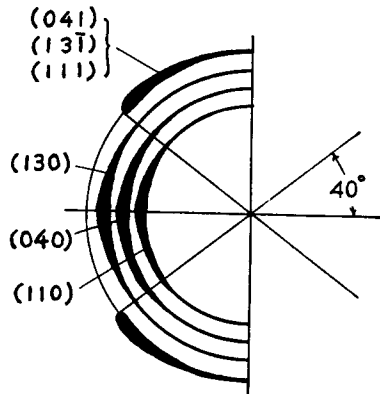


Fig. 6. Diffraction pattern (\parallel) of the uniplanar oriented film expected from a stereographic projection.

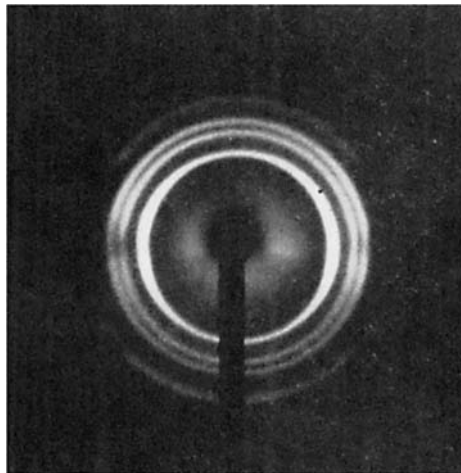


Fig. 7. X-ray diffraction photograph (\parallel) obtained with a model film of uniplanar orientation.

be distinguished from the (040) selective uniplanar orientation, because n_α is equal to n_β in the case of polypropylene.

The diffraction pattern with the beam parallel to film with uniplanar orientation can be expected to be as shown in Figure 6 by means of a stereographic projection. In order to confirm this, a model film must be used, because the orientation of a highly polyaxially stretched film is not purely uniplanar but it is contaminated with some fraction of the selective uniplanar orientation (040). A strip of isotropic film was uniaxially stretched $7\times$ at 130°C ., and a value of 30×10^{-3} for Δn was obtained. It was found in the previous paper in this series that such a strip is monoaxially oriented. Therefore when this film is rolled into a cylindrical rod around the ps axis and an x-ray photograph is taken with the x-ray beam

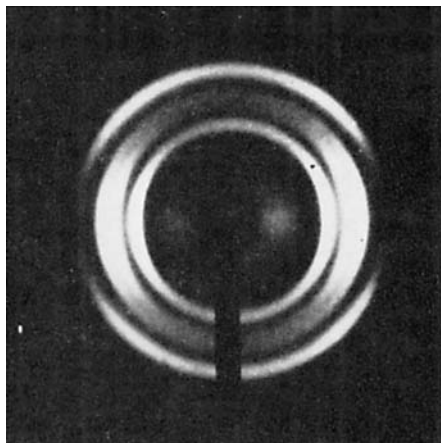


Fig. 8. X-ray diffraction pattern (\parallel) of a two-step biaxially stretched film.

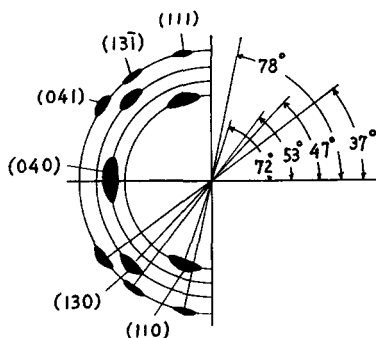


Fig. 9. Expected diffraction pattern (\parallel) of a film of selective uniplanar (040) orientation.

perpendicular to the rod axis, the pattern is equivalent to that from a film of the uniplanar orientation. The observed pattern is in accord with this expectation, as shown in Figure 7. The pattern is very akin to that shown in Figure 6, except for a slightly irregular intensity distribution near the equator which may be an artifact, because no such irregularity appeared in a repeated test.

Figure 8 shows the x-ray photograph of a two-step biaxially stretched film (150% stretching, 100% restretching, nearly balanced), where the incident x-ray beam was parallel to the *ps* axis. When the x-ray beam was parallel to the *pp* axis too, a closely similar pattern was obtained. This is further evidence for the uniplanar orientation of this sort of film.

If the (040) is selectively uniplanar, a pattern of the type shown in Figure 9 would be expected. The actually observed patterns (Figs. 5e-5g), are considered to be the overlaps of these two types of pattern. According to Figures 6 and 9, the (111) + (131) + (041) diffraction must range from $\phi = 40-90^\circ$, and this is found, as shown by Figures 5e-5g. It can be concluded, therefore, that as the polyaxial stretching proceeds, the film

approaches a uniplanar orientation and at the same time a progressively increasing fraction of the (040) planes become parallel to the film surface.

Figures 5f, 5f' and 5g, 5g' are x-ray photographs of the films stretched with the apparatus A at 130°C. and with the apparatus B at 100°C., respectively. They are prominently selective uniplanar, and the diffractions, with the beam perpendicular to the film, for (040) and (130) are correspondingly very weak. This type of orientation is likely to be more pronounced at lower temperatures.

This phenomenon leads us to the consideration that selective uniplanar orientation is apt to occur on stretching with restraint of the molecular motion around the stretching axis. The observation in the previous and the above studies that this type of orientation did not appear during the two-step biaxial stretching is illustrated by the stretching without perpendicular constraint.¹ On the contrary, one-step biaxial stretches brings about marked selective uniplanar orientation. Even in polyaxial stretching, insufficient constraint in the early stage of low v_A brought about only the uniplanar orientation as indicated in Figure 5. So it is expected that the selective uniplanar orientation is caused by pressing or rolling, as has been described by Sobue and Tabata¹¹ and Wilchinsky.¹²

Degree of Orientation of Crystalline and Amorphous Regions

Δn_{ss} is divided into a contribution from the crystalline region, $X\Delta n_{ssc}$ and that from the amorphous region, $(1 - X)\Delta n_{ssa}$ as described in eq. (4) (see Fig. 10).

$$\begin{aligned}\Delta n_{ss} &= X \Delta n_{ssc} + (1 - X)\Delta n_{ssa} \\ &= X f_x \Delta n_c^0 + (1 - X)f_a \Delta n_a^0\end{aligned}\quad (4)$$

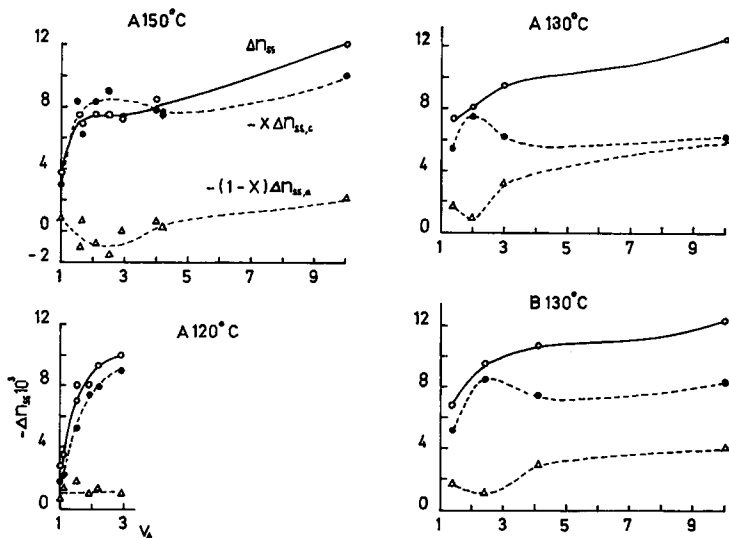


Fig. 10. Contributions of the crystalline and the amorphous regions to Δn_{ss} . A and B denote stretchings with the apparatus A and B, respectively.

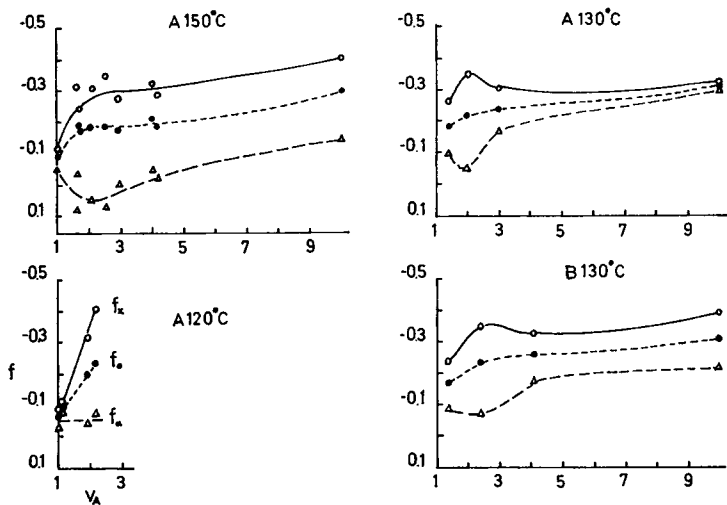


Fig. 11. Degree of orientation of crystalline and amorphous regions.

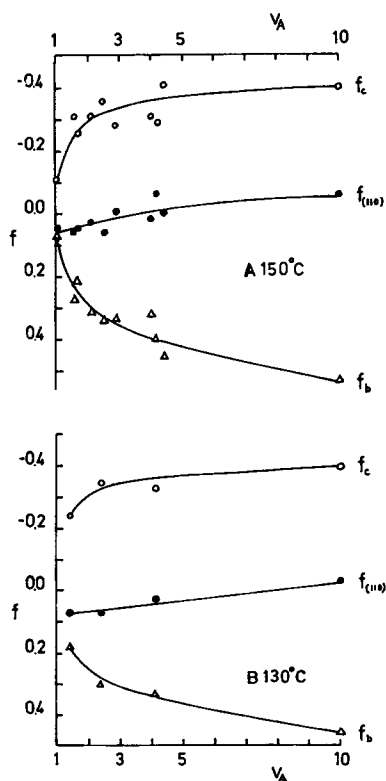


Fig. 12. Change in the orientation of the crystalline axis during stretching.

Here X is the crystalline fraction calculated from the density, f_x and f_a are the c axis orientation degrees in the crystalline and the amorphous regions, respectively, relative to the ss axis. f_x can be calculated by applying the Wilchinsky's principle, because the orientation within the film is symmetrical around the ss axis. The condition $n_\alpha = n_\beta$ allows application of eq. (4) to the present films although they are selective uniplanarly oriented.

In all cases the contribution from the crystalline region is predominant and the amorphous contribution is small, especially when the stretching is carried out at elevated temperatures because of the larger relaxation.

Figure 11 is another expression of Figure 10 in terms of the orientation degree f . From the fact that the final value of f_x is -0.4 , it can be seen that the c axis in the crystalline region lies almost completely parallel to the film surface. On the other hand, the molecule axis is randomly oriented in the amorphous region. Such an orientation of the c axis proceeds along with the partial orientation of the b axis perpendicularly to the film surface (Fig. 12), while the a axis apparently remains almost unoriented.

It is noteworthy that a shallow minimum appears on the f_a curve at the early stage of polyaxial stretching also (Fig. 11); similar results were obtained by Stein et al.¹³ for low-density polyethylene and Okajima and Kurihara¹⁴ for polypropylene in the case of monoaxial stretching.

Comparison of Polyaxial Stretching with the Two-Step Biaxial Stretching

Two-step biaxial stretching was already reported.¹ The data for the biaxially balanced film from that study are compared with those of the polyaxial stretching described above in Table II.

In Figure 13, B100, B130, and B160 indicate Δn_{ss} versus ν_A for biaxial stretchings at 100, 130, and 160°C., respectively, and the curves P100, P130, and P150 are those for polyaxial stretchings at 100, 130, and 150°C., respectively. This figure shows that two-step biaxial stretching is more effective for orienting the molecules than polyaxial stretching, due to the leveling off of the latter curve. However it is interesting that the final

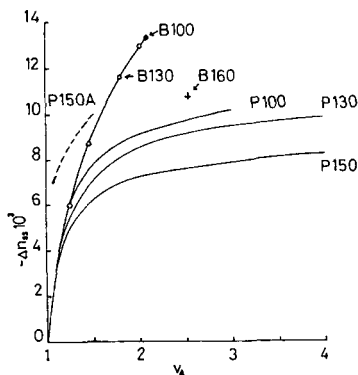


Fig. 13. Comparison between the orientation behaviors during two-step biaxial stretching (B100, B130, B160) and the polyaxial stretching (P100, P130, P150).

TABLE II
 Data on Biaxially Balanced Films*

Temperature of stretching, °C.	λ_{12} , %	λ_2^0 , %	$-\Delta n_{ss}$ $\times 10^3$	v_A , \times area expanded	d , g./cm. ³
100	200	120	13.1	1.90	0.9083
130	50	40	5.5	1.22	0.9073
130	100	72	8.7	1.39	0.9086
130	200	120	11.8	1.75	0.9079
130	300	140	12.6	3.12	0.9072
160	700	120	10.3	4.55	0.9114

* Data from Part I of this series.¹

value of $-\Delta n_{ss}$ is 13×10^{-3} in both types of stretching. This is because restretching becomes very difficult due to the tendency for the film to split when λ_{12} , first-step stretching, is made too large (done to lower n_{ss} drastically). v_A cannot be made much larger than 2 in the case of the biaxial stretching, while in the alternative type of stretching v_A easily reaches values of 15–20. Of course the detailed fine structure of the film is different depending on the type of stretching even when the Δn_{ss} values are equal.

These studies indicate that birefringence value of -13×10^{-3} appears to be a critical value for Δn_{ss} but the maximum value of Δn_{ss} obtained experimentally may be a function of the fine structure of the film, depending on crystallinity, molecular weight and molecular weight distribution, tacticity, etc. Precise future studies are required to determine the effects of these factors.

The authors wish to thank the Ministry of Education for a grant-in-aid for fundamental scientific research. We are also grateful to the Chisso Corporation for kindly supplying film used in this study.

References

1. S. Okajima, K. Kurihara, and K. Homma, *J. Appl. Polymer Sci.*, **11**, 1703 (1967).
2. Z. W. Wilchinsky, *J. Appl. Phys.*, **31**, 1969 (1960); *J. Appl. Polymer Sci.*, **7**, 1 (1963).
3. D. A. Keedy, J. Powers, and R. S. Stein, *J. Appl. Phys.*, **31**, 1911 (1960).
4. K. G. Denbigh, *Trans. Faraday Soc.*, **36**, 936 (1940).
5. C. W. Bunn and R. Daubeny, *Trans. Faraday Soc.*, **50**, 1173 (1954).
6. R. J. Samuels, *J. Polymer Sci. A.*, **3**, 1741 (1965).
7. S. Kuribayashi and A. Nakai, *Sen-i Gakkaishi*, **18**, 64 (1962).
8. N. Yamada, N. Kishi, and Z. Orito, paper presented at a meeting of the Society of Polymer Science, Japan, November 1964.
9. J. Padden and H. D. Keith, *J. Appl. Phys.*, **30**, 1479, 1485 (1959).
10. O. Ishizuka, *Sen-i Gakkaishi*, **18**, 198 (1962).
11. H. Sobue and Y. Tabata, *J. Appl. Polymer Sci.*, **2**, 62 (1959).
12. Z. W. Wilchinsky, *J. Appl. Polymer Sci.*, **7**, 923 (1963).
13. S. Hoshino, J. Powers, D. G. LeGrand, H. Kawai, and R. S. Stein, *J. Polymer Sci.*, **58**, 185 (1962).
14. S. Okajima and K. Kurihara, *Sen-i Gakkaishi*, **22**, 351 (1966).

Received March 10, 1967

Revised May 16, 1967